Sequential analysis of diamond nucleation on silicon (001) with bias enhanced nucleation using X-ray photoelectron spectroscopy and reflection high energy electron diffraction investigations

C. Sarrieu, N. Barth, A. Guise, Jean-Charles Arnault, Samuel Saada, S. Barrat, E. Bauer-Grosse

Sequential analysis of diamond nucleation on silicon (001) with bias enhanced nucleation using X-ray Photoelectron Spectroscopy and Reflection High Energy Electron Diffraction investigations.

C. Sarrieu*[1], N. Barth[1], A. Guise[1], J.C. Arnault[2], S. Saada[2], S. Barrat[1], E. Bauer-Grosse[1]

[1] IJL UMR 7198, CP2S, Équipe Élaboration et Fonctionnalité de Couches Minces, École des Mines de Nancy, Parc de Saurupt, F-54042 NANCY, France.
[2] CEA, LIST, Diamond Sensors Laboratory, F-91191 GIF-SUR-YVETTE, France.

Diamond synthesis by Microwave Plasma assisted Chemical Vapour Deposition (MPCVD) with a Bias Enhanced Nucleation (BEN) step constitutes the most efficient method to obtain heteroepitaxy and is also useful to reach high nucleation densities. In this study, sequential Reflection High-Energy Electron Diffraction (RHEED) and X-ray Photoelectron Spectroscopy (XPS) investigations enabled us to highlight the formation of amorphous carbon and crystalline silicon carbide on the surface before diamond growth. By varying the bias voltage, we underlined an optimized value corresponding to a higher quantity of amorphous carbon. This quantity is strongly correlated to the diamond nucleation density. As for the quality of the SiC texture, this seems to be directly linked to bias voltage too: low bias voltages enable us to obtain high oriented 3C-SiC whereas high bias voltages lead to a completely misoriented polycrystalline SiC film.

Introduction:

In the case of diamond heteroepitaxy on silicon, the chemical and structural properties of the substrate surface before nucleation is of great importance for the quality of diamond films [1, 2]. Some works have demonstrated that native silicon oxide can be removed by a H_2 or H_2-CH_4 plasma step [3-6]. However, H_2 plasma cannot be described as a simple etching step and in fact it is difficult to prevent carbon/silicon interactions because of the carbon contamination [7, 8]. During diamond synthesis using MPCVD, the carbon/silicon interactions, also called carbonisation phenomena, lead to the formation of a $Si_{1-x}C_x$ transition layer which is not completely controlled [9, 10]. Moreover, some studies have exhibited that this carbonisation has a strong influence on diamond nucleation due to the possible formation of a 3C-SiC buffer layer which can favour the oriented diamond nuclei [2, 11]. Diamond epitaxy strongly depends on the structural nature of this buffer layer and on the BEN conditions [12]. The present work is devoted to the characterisation of the transformed silicon surface during the successive steps leading to diamond nucleation by MPCVD using BEN. In this study, RHEED and XPS allowed us to correlate both chemical and crystalline surface transformations. The quantity of amorphous carbon and the evolution of the silicon carbide texture were particularly investigated by tuning the bias voltage.

Experiments

The experimental set-up is presented elsewhere [13]. We started from 10×10 mm^2 samples cut from (001) silicon wafers. Samples were prepared by ultrasonic cleaning, preheating under vacuum, a H_2 plasma step and a BEN step. Ultrasonic cleaning is made *ex situ* in acetone, then in ethanol. The *in situ* silicon preheating is allowed by HF induction heating of the graphite substrate-holder. Then the hydrogen plasma is obtained by microwave excitation. The BEN consists in a very short (30 s and 60 s) cathodic bias of the substrate under H_2/CH_4 plasma in relation to a molybdenum anode located above the substrate.
For the sequential study, five samples were performed with the A process (Table 1). The surface treatment was stopped after each different step (cleaning, preheating, H2 plasma, 30 s and 60 s of BEN). The samples were then investigated by XPS and RHEED.
In order to study by XPS the evolution of the chemical surface state according to different bias voltages, three other samples were synthesized using the same A process with 60, 140 and 180 V bias voltages.
Another serie of three samples was prepared with the B process at 100, 130 and 160 V bias voltages. The surface structure obtained with both processes were analyzed by RHEED and compared.

Steps	Duration (s)	Pressure (hPa)	CH_4 / H_2 (%)	P_{wave} (W)	Bias Voltage (V)	Temperature (°C)
"A Process" (RHEED and XPS investigations)						
Preheating	300	10^{-3}	-	-	-	550
H_2 plasma	60	20	0 / 100	600	-	850
BEN	30 – 60	13	5 / 95	400	60-100-140-180	820
"B Process" (only RHEED investigations)						
Preheating	480	18	0 / 100	-	-	670
H_2 plasma	300	18	0 / 100	460	-	925
BEN	60	18	5 / 95	460	100-130-160	925

Table 1 Experimental parameters.

All RHEED patterns were obtained *ex situ* with a mono-energetic beam of 30 keV. Small incident angles of 0.2 - 3° were used to explore few angstroms beneath the silicon surface while islands formed on top could be investigated. All the sample width along the beam direction contributes to the pattern. XPS measurements were performed with a monochromatic Al K_α source (FWHM of 0.25 eV). The binding energy scale was calibrated versus the Au 4f 7/2 peak located at 83.6 eV.

Results and discussion:

1) Sequential analysis of the process:

Preheating under vacuum

No surface chemical transformations can be noticed by XPS during this step. The Si 2p spectrum (Fig. 1a) shows two other contributions beside the elemental silicon peak. One is attributed to SiO_x (substoichiometric oxides with $0<x<2$) at 102.8 eV, the other to SiO_2 at 103.5 eV. They constitute the native oxide layer on the silicon surface [6, 14]. On the other hand, the spectrum in the C 1s region (Fig. 1b) shows a wide peak centred at 284.9 eV which is attributed to a carbonaceous contamination.

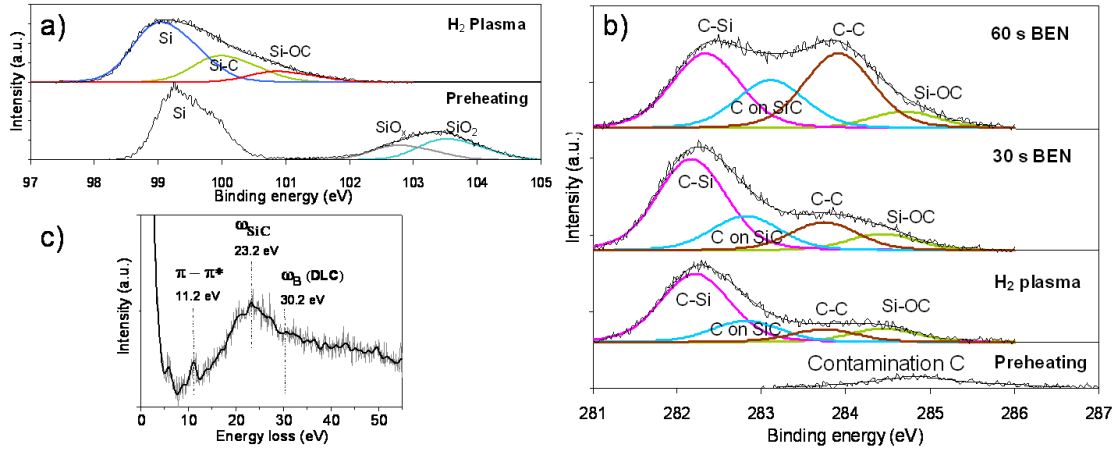

Fig. 1 XPS sequential analysis: Si 2p region after preheating and H_2 plasma (a); C 1s region after preheating, H_2 plasma, 30 s and 60 s of BEN (b). XEELS spectrum in C 1s region after BEN at 100V (c).

The RHEED pattern obtained after preheating with the electron beam along the [100] azimuth of the silicon substrate do not show any surface transformations either (Fig. 2a). But in this case, the observation of the silicon with a smaller incident angle failed: this confirms the presence of the amorphous native oxide layer.

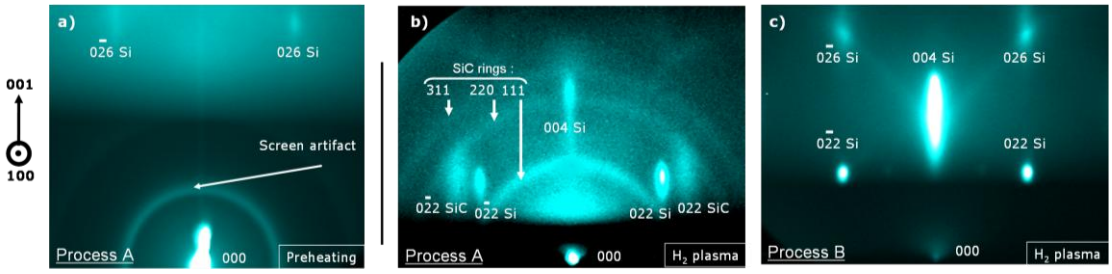

Fig. 2 RHEED sequential analysis of A process: patterns after preheating (a) and after H_2 plasma (b). (c) corresponds to the silicon surface after a H_2 plasma in the case of the B process.

Hydrogen plasma step

We can estimate the efficiency of this step in removing the native oxide in Fig. 1-a. Indeed, we can see that the peaks associated to SiO_x are absent. On the other hand, two additional peaks located at 100 eV and 100.8 eV are assigned to silicon carbide [14] and silicon oxycarbide formation [15] respectively. This is in good agreement with the C 1s core level (Fig. 1b) where an intensive peak at 282.2 eV and a less intensive at 284.4 eV underline the respective contributions of C-Si bond [14] and C-SiO bond [16]. Moreover, a peak at 282.8 eV most probably shows a rearrangement of carbon on 3C-SiC [17], while the presence of C-C bonds is highlighted by a peak at 283.7 eV [14, 17]. However the peak of contamination carbon observed at the previous stage has disappeared.

The RHEED pattern obtained after a H_2 plasma (Fig. 2b) with a small incident angle presents the formation of new crystalline structures. The signal is difficult to observe, so the sharpness of the picture has been enhanced by image processing. The large spots obtained can be indexed as (0-22) and (022) 3C-SiC. The spot shapes are sensitive to the film microstructure [19]. Their

height in particular is inversely proportional to the depth of the electron penetration. In our case, the noticeable height of the SiC diffraction spots suggests a low penetration. This could be associated with a quite flat surface of heteroepitaxial SiC. As for the three thin rings, they correspond to the {111}, {220} and {311} interplanar spacings of 3C-SiC and suggest the presence of misoriented SiC islands. By moving the electron beam in relation to the sample, the rings disappear evoking a SiC heterogeneous distribution. Both types of SiC were probably formed by different mechanisms. The H_2 plasma has not only an etching role (native oxide) since chemical modifications occur on the silicon surface when the carbon contamination is present. Parameters of the B process were optimized to prevent the formation of silicon carbide during the hydrogen plasma step. The *in situ* RHEED pattern in Fig. 2c does not reveal any SiC structure with this last process. The silicon signal is more intense and its pattern is composed of long rods. This suggests that the native oxide layer has been removed and that the silicon surface has remained flat enough to allow 2D diffraction. However, the carbon contamination must be present too in this case, but the higher temperature obtained during the H_2 plasma step probably induces a stronger etching of the surface preventing the formation of SiC.

BEN step at 100V

According to the peak areas extracted from Fig. 1b, the C-C bond contribution increases with BEN time. Starting from 11% of the global C 1s area after etching, it rises to 17% after 30 s and up to 35% after 60 s. As a consequence, the C-Si bond contribution decreases.

An X-ray Electron Energy Loss Spectrum (XEELS) recorded from the 100 V bias voltage sample (Fig. 1c) allows us to confirm the presence of silicon carbide. The corresponding plasmon is located at 23.2 eV from the C-Si peak [18]. Moreover, the presence of a feature at 11.2 eV (9.7 eV from the C-C peak) and of a shoulder at 30.2 eV (28.7 eV from the C-C peak) suggests the existence of a diamond-like carbon phase [16]. Nevertheless, the spectrum does not reveal any diamond at this stage, the main observed signature for C-C bonds is amorphous carbon. However, diamond nuclei must be present too since diamond islands have been grown by CVD from this step (Fig. 3b).

The RHEED patterns (Fig. 4b) obtained with a beam along the [100] Si substrate present diffraction arcs corresponding to (004), (022) and (02-2) of 3C-SiC. This means that an out-of-plane orientation distribution exists in the SiC cover layer. The absence of a pattern related to a crystallized carbon phase (as graphite and/or diamond) supports the idea of the main presence of amorphous carbon on the surface.

2) Influence of the bias voltage value

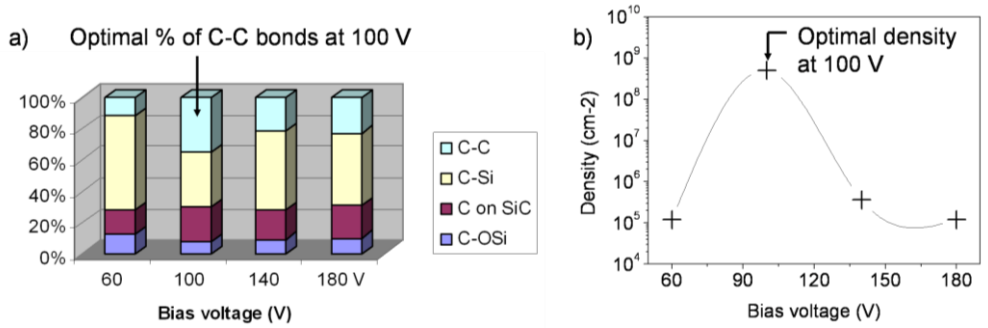

Fig. 3 Percentages of the different carbon binding states extracted from C 1s for different bias voltages (a). After growth: variation of the diamond nuclei density according to the bias voltage (b).

C 1s XPS spectra were fitted and the percentage for each binding state was calculated (area of the considered fitting peak over area of the global C 1s peak). The evolution of the carbon binding states is reported in Fig. 3a versus the bias voltage. Slight variations in the proportion of the carbon rearranged on SiC and in oxycarbide are thus observable but they do not seem significant. However the SiC and the amorphous carbon phase seem to compete. In particular, we observe at 100 V that the C-C bonds proportion is maximum and rises to 35% while the C-Si proportion (around 18%) is minimum. In the same way, the XPS C 1s spectra recorded by Y. Ma et al. [20] for different bias voltages (their process parameters are similar to our A process, but the proportion of methane is 30%) show a contribution around 104.5 eV which is maximal at 100 V and seems to be amorphous carbon.

In order to link this result with nucleation density, the samples were subjected to 30 min of an additional growth step (13 hPa, 1% of methane in hydrogen, microwave power at 400 W). Thus the nucleation density became estimable by SEM. Figure 3b shows the density evolution according to the bias. The curve reveals a maximum value of 5.10^8 cm^{-2} at 100 V instead of around 10^5 cm^{-2} in the other cases. Such behaviour of the density curve is in agreement with previous studies [20-22]. J. Gerber et al. [21] link this evolution to the variation of the kinetic energy of ions that they measure by retarding field probe.

In our case and in the Ma et al. study [20] as well, the maximum density coincides with a maximum of amorphous carbon proportion. Thus these two phenomena seem to be correlated and to be optimal for a certain kinetic energy of the accelerated ions. However, the proportion of epitaxial diamond crystallites could vary differently. For example, Thürer et al. [12] have shown an increase in the diamond in-plan misorientation with the bias value.

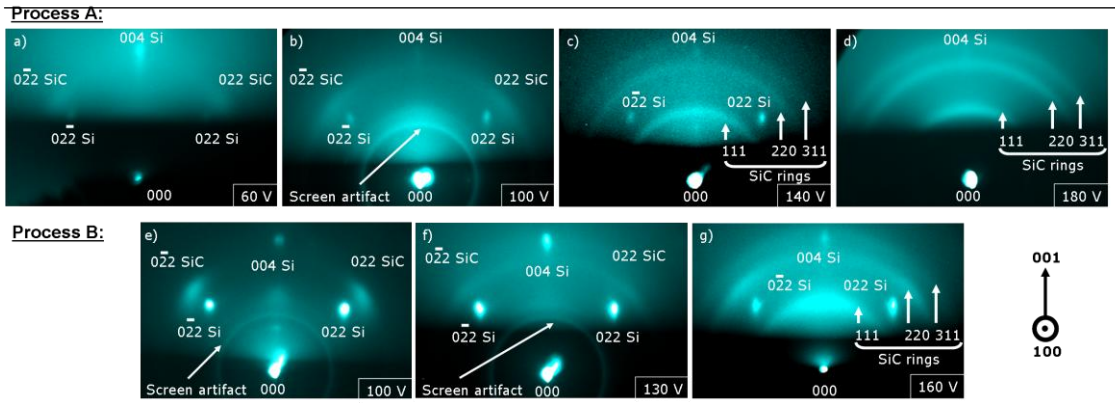

Fig. 4 Evolution of the RHEED patterns with the bias voltage after BEN. (a), (b), (c), (d) performed with the A process, (e), (f), (g) performed with the B process.

RHEED investigations allow us to focus on the influence of the bias value on SiC structures. In this study all patterns were performed with an electron beam along the Si [001]. The samples obtained with the A process (Fig. 4a, b, c, d) are compared here with these ones obtained with the B process (Fig. 4e, f, g). We remind that, for the A process, some SiC microstructures can have been produced already in the step preceding the bias, whereas this is not the case with the B process.
Concerning the samples obtained with the A process, RHEED exhibits a structure evolution according to the bias voltage. After a 60 V bias, diffuse 3C-SiC spots can be detected despite the inelastic scattering background. Such spots are 3D diffraction and can be associated with the presence of very oriented 3C-SiC islands. As for the strong background noise, it is probably due to some amorphous materials on the surface. Concerning the patterns obtained in the same conditions after 140 V and 180 V bias voltages, they are therefore composed of rings indicating totally misoriented islands. The fact that the silicon signal has completely disappeared from all beam orientations beyond 180 V seems to signify that in these drastic conditions, the SiC very quickly grows and that it can completely cover the whole silicon surface. As for the 100 V sample, it presents an intermediate pattern: we notice arc-shaped spots which mean that the SiC islands have a preferential orientation.
Concerning the sample prepared with the B process, similar evolutions are observable. Very reduced arc-shaped spots of 3C-SiC are obtained after a 100 V bias whereas SiC ring patterns appear at 160 V. The 140 V bias is an intermediate situation.
Higher bias voltages give higher kinetic energies to the ions [21], so the evolution of the RHEED patterns according to the bias voltage seems to show that high kinetic energies of ions are responsible for the degradation of the 3C-SiC texture quality. This was observed for both processes, even if the A process leads to the heterogeneous formation of some SiC microstructures before the BEN. Consequently, the potential carbon contamination before the BEN only concerns a small part of the surface, and the SiC is mainly formed during the BEN in both cases. Furthermore, the BEN parameters of the A and B processes have been chosen quite different. In particular, the pressure has been increased of 40% and the temperature is 12% higher. As a result, the very strong influence of the bias value on the orientation of the silicon carbide islands must be valid in a large parameter window.

Conclusion

The silicon/diamond interface is formed during the first stages of diamond nucleation using BEN-MPCVD. A H_2 plasma before the bias step removes the native oxide. But the presence of carbon contamination can lead to locally deposit oriented or misoriented silicon carbide on the silicon surface. During the bias step, diamond nuclei are produced but this phenomenon competes with the formation of amorphous carbon material and silicon carbide which cover the surface. Their relative proportion on the surface seems to be linked to the bias voltage. Moreover, the diamond nuclei density and the quantity of amorphous carbon are optimal for the same bias value (100 V in our case). Concerning the SiC, it grows as islands of 3C-SiC and covers the surface during the bias step. It forms a buffer layer whose orientation quality decreases with the bias voltage and thus with the kinetic energy of the accelerated ions. Previous studies have shown that the orientation quality of this SiC film has a strong impact on diamond nucleation. The synthesis of the SiC buffer layer should be prepared with other methods before the bias step or at a low bias voltage value. We will investigate the characteristics of such a film and link them to diamond epitaxy in a next study.

References

[1] S.D. Wolter, D. Borca-Tasciuc, G. Chen, J.T. Prater, and Z. Zitar, Thin Solid Films **469-470**, 105 (2004).
[2] T. Suesada, N. Nakamura, H. Nagasawa, and H. Kawarada, Jpn. J. Appl. Phys. **34**, 4898 (1995).
[3] R. Stoner, G.H.M. Ma, S.D. Wolter, and J.T. Glass, Phys. Rev. B **45**, 11067 (1992).
[4] F. Arezzo, N. Zacchetti, and W. Zhu, J. Appl. Phys. **75**, 5375 (1994).
[5] R. Stöckel, K. Janischowsky, S. Rohmfeld, J. Ristein, M. Hundhausen, and L. Ley, J. Appl. Phys. **79**, 768 (1996).
[6] S. Saada, J.-C. Arnault, N. Tranchant, M. Bonnauron, and P. Bergonzo, Phys. Stat. Sol. (a) **204**, 2854 (2007).
[7] S. Barrat, A. Guise, A. Aouni, M. Diani, and E. Bauer-Grosse, Diamond Relat. Mater. **17**, 428 (2008).
[8] P. Mahalingam, and D. S. Dandy, Thin Solid Films **322**, 108 (1998).
[9] J. Wei, J. Ahn, and CL. Hing, Crystal Research and Technology **33**, 441 (1998).
[10] M. Schreck, F. Hörmann, H. Roll, T. Bauer, and B. Stritzker, New Diamond Front. Carbon Technol. **11**, 189 (2001)

[11] T. Suzuki, and A. Argoitia, Physica Status Solidi (a) **154**, 239 (1996).
[12] K.-H. Thürer, M. Schreck, and B. Stritzker, Phys. Rev. B **57**, 15454 (1998)
[13] S. Barrat, S. Saada, J.M. Thiebaut, and E. Bauer-Grosse, Diamond Relat. Mater. **10**, 1637 (2001).
[14] L. Demuynck, J.C. Arnault, R. Polini, and F. Le Normand, Surf. Sci. **377-379** 871 (1997).
[15] Y. Hijikata, H. Yaguchi, M. Yoshikawa and S. Yoshida, Appl. Surf. Sci. **184**, 161 (2001).
[16] S. Rey, F. Antoni, B. Prevot, E. Fogarassy, J.C. Arnault, J. Hommet, F. Le Normand and P. Boher, Appl. Phys. A **71**, 433 (2000)
[17] J.-C. Arnault, L. Demuynck, C. Speisser, and F. Le Normand, Eur. Phys. J. B **11**, 327 (1999).
[18] R.J. Meilunas, R.P.H. Chang, S. Liu, M.M. Kappes, Appl. Phys. Lett. **59**, 3461 (1991).
[19] R. T. Brewer and Harry and A. Atwater, J. Appl. Phys. **93**, 205 (2003).
[20] Y. Ma, T. Tsurumi, N. Shinoda and O. Fukunaga Diamond Relat. Mater. **4**, 1325 (1995).
[21] J. Gerber, S. Sattel, H. Ehrhardt, J. Robertson, P. Wurzinger and P. Pongratz, J. Appl. Phys. **79**, 4388 (1996).
[22] A. Guise, S. Barrat and E. Bauer-Grosse, Diamond Relat. Mater. **16**, 695 (2007).